

Neural Ordinary Differential Equations for Intervention Modeling

Daehoon Gwak,¹ Gyuhyeon Sim,² Michael Poli,² Stefano Massaroli,³ Jaegul Choo,² Edward Choi²

¹ Korea University, ² KAIST, ³ The University of Tokyo

hune282@korea.ac.kr, {ghsim, poli_m, jchoo, edwardchoi}@kaist.ac.kr, massaroli@robot.t.u-tokyo.ac.jp

Abstract

By interpreting the forward dynamics of the latent representation of neural networks as an ordinary differential equation, Neural Ordinary Differential Equation (Neural ODE) emerged as an effective framework for modeling a system dynamics in the continuous time domain. However, real-world systems often involves external interventions that cause changes in the system dynamics such as a patient being administered with particular drug. Neural ODE and a number of its recent variants, however, are not suitable for modeling such interventions as they do not properly model the observations and the interventions separately. In this paper, we propose a novel neural ODE-based approach (IMODE) that properly model the effect of external interventions by employing two ODE functions to separately handle the observations and the interventions. Using both synthetic and real-world time-series datasets involving interventions, our experimental results consistently demonstrate the superiority of IMODE compared to existing approaches.

1 Introduction

Although we live in continuous time, physical systems (*e.g.*, bouncing ball, patient state) are often observed in a discretized fashion, either regularly or irregularly. For example, while climate sensors can collect information at every hour, patient blood samples are drawn only by a physician’s order. Various approaches have been proposed to handle such time-series data with neural networks, often modifying recurrent neural networks (RNNs) with varying degrees of success (Choi et al. 2016; Du et al. 2016; Lipton, Kale, and Wetzel 2016; Baytas et al. 2017; Che et al. 2018), until Neural Ordinary Differential Equations (Neural ODEs) (Chen et al. 2018) proposed a natural framework to model a system dynamics in a continuous time domain.

Neural ODEs view the forward pass of the vector representation \mathbf{h} , often corresponding to the system state, as numerically solving an ordinary differential equation using the time derivative $\dot{\mathbf{h}} := d\mathbf{h}/dt$ parameterized by a neural network. As this framework provides a natural means to handle both regular as well as irregular time-series data, previous studies have extended Neural ODEs to encode observation sequences. These approaches have demonstrated improved

Preprint. Under review.

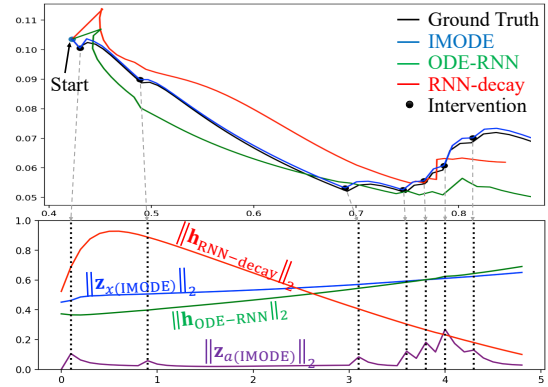


Figure 1: (Top) In a 2D plane, IMODE, ODE-RNN and RNN-Decay simulate a trajectory intervened by time-decaying effects. (Bottom) X-axis indicates time while Y-axis denotes L_2 norm of hidden-state vectors. IMODE separately models the autonomous dynamics ($\|\mathbf{z}_x(\text{IMODE})\|_2$) and the intervention effect ($\|\mathbf{z}_a(\text{IMODE})\|_2$) (see Figure 2), while ODE-RNN and RNN-Decay fail to handle the interventions correctly.

performance in prediction tasks on simulated data, climate records, and medical records (Rubanova, Chen, and Duvenaud 2019; De Brouwer et al. 2019; Jia and Benson 2019; Poli et al. 2019).

Real-world systems, however, are often influenced by external factors (*i.e.* interventions), such as a patient being administered some medication at a particular time. Depending on the system characteristic, these influences can change the system dynamics instantaneously or in a prolonged manner. While effective in modeling intervention-free dynamics, previous approaches capable of handling discrete or continuous feature evolution such as RNN-decay, GRU-D, and ODE-RNNs (Che et al. 2018; Rubanova, Chen, and Duvenaud 2019) were not designed to handle cases with external interventions. In particular, ODE-RNNs and their derivative architectures (De Brouwer et al. 2019; Jia and Benson 2019) place a strong assumption on the effect of additional observations on the system state; by aggregating input information with either recurrent cells or a multi-layer perceptron (MLP), the system state is directly modified by each observations.

In response, this paper proposes Intervention-Modeling Or-

dinary Differential Equation (IMODE) which aims to model systems with (regular or irregular) interventions. Unlike alternative approaches, IMODE is designed to handle interventions that affect the system dynamics in various ways. Specifically, we employ two separate ODE functions, where one is tasked with learning the autonomous dynamics from a sequence of observations, and the other is tasked with learning the effects of external forces on the system. Delegating the task of modeling the intervention effect to a separate component ultimately leads to a disentangled, interpretable model. When an external force is applied, this separate component alters the system’s dynamics, instead of altering the state directly.

The contribution of this paper is summarized as follows:

- We propose a new framework IMODE for modeling interventions using Neural ODEs, where one component is dedicated to learning autonomous dynamics, while a separate module tracks the effect of external interventions. We provide specific examples of systems with different intervention types (*e.g.*, permanent, decaying) and describe how IMODE can be implemented per different systems.
- Using synthetic datasets and real-world medical records, we not only show IMODE consistently outperforms previous approaches for intervention modeling, but also analyze IMODE’s behavior to show it is separately learning the autonomous dynamics and the intervention effects as intended.

2 Background and Motivations

This section briefly reviews Neural ODEs along with the definition of necessary notations. We then motivate our work by discussing the limitation of existing approaches in intervention modeling.

Neural ODEs The Neural ODEs provide a general framework for modeling the continuous transformation of the state (*i.e.* latent representation \mathbf{h}) by assuming the state dynamics can be modeled by an ordinary differential equation. Neural ODEs parameterize the derivative of the state (*i.e.* system dynamics $d\mathbf{h}/dt$) with a neural network f_θ as

$$\dot{\mathbf{h}} = f_\theta(t, \mathbf{h}(t)), \quad \mathbf{h}(t_N) = \mathbf{h}(t_0) + \int_{t_0}^{t_N} f_\theta(\tau, \mathbf{h}(\tau)) d\tau \quad (1)$$

Given an initial state vector $\mathbf{h}(t_0) \in \mathbb{R}^{n_h}$, generally corresponding to the input vector $\mathbf{x} \in \mathbb{R}^{n_x}$ or its embedding, the system state $\mathbf{h}(t_k)$ is obtained by integrating forward the vector field $f_\theta : \mathbb{R} \times \mathbb{R}^{n_h} \times \mathbb{R}^{n_\theta} \rightarrow \mathbb{R}^{n_h}$, parameterized by $\theta \in \mathbb{R}^{n_\theta}$. While we consider θ to be constant over time, the discussion below is directly compatible with time-varying parameters (Massaroli et al. 2020b).

Impulsive Systems Motivated by Neural ODEs’ flexibility to model time-series data, several approaches extended the Neural ODE framework to encode a sequence of observations $\{\mathbf{x}_k\}$, whether being regular or irregular. ODE-RNN (Rubanova, Chen, and Duvenaud 2019) uses the RNN to encode a sequence of observations, where the latent state \mathbf{h} flows according to an ODE between observations, and a new

observation \mathbf{x}_k directly modifies \mathbf{h} according to the RNN update equation. GRU-ODE-Bayes (De Brouwer et al. 2019) specifically uses the GRU (Cho et al. 2014) to encode observations, where a new observation directly modifies \mathbf{h} according to the GRU update equation combined with some masking operations. Neural Jump Stochastic Differential Equations (NJSDE) (Jia and Benson 2019) combines ODEs with point processes to model stochastic events. In NJSDE, given a new observation, an event history representation is directly modified via an MLP, combining some internal state with the observation.

Let (\mathcal{T}, \succeq) be a finite linearly ordered set, called the *data time* set (typically $\mathcal{T} = \{t_0, t_1, \dots, t_N\}$). We assume an *input-output data stream* is given as a sequence $\{x_{t_k}\}_{t_k \in \mathcal{T}}$. For a compact notation, we denote \mathbf{x}_{t_k} with \mathbf{x}_k . The underlying core approach in all three approaches is to update the system state \mathbf{h} via a particular non-linear operation when a new observation is given, which can be generalized as an *impulsive differential equation* (Lakshmikantham, Simeonov et al. 1989; Kulev and Bainov 1988) of the type,

$$\begin{cases} \dot{\mathbf{h}} = f_\theta(t, \mathbf{h}(t)) & t \neq t_k \\ \mathbf{h}^+ = g_\phi(\mathbf{h}(t), \mathbf{x}_k) & t = t_k \end{cases} \quad \text{for } t_k \in \mathcal{T}, \quad (2)$$

where \mathbf{h}^+ indicates the value of \mathbf{h} after the discrete jump at t_k . Between observations, the system state \mathbf{h} evolves according to continuous dynamics. New observations, on the other hand, trigger a jump of \mathbf{h} to \mathbf{h}^+ as determined by g_ϕ . For the rest of the paper, we refer to this broad family of models as *Neural Jump Differential Equations* (NJDE).

Although it is possible to use NJDEs to naively model systems with interventions, by, say, simply concatenating them with observations, this approach is limited as it does not explicitly separate autonomous dynamics of the system from these effects. This, in turn, makes it challenging to properly reconstruct the evolution of a system subject to external forces.

It should be noted that according to Eq. 2, new inputs to NJSDEs induce state jumps. In general, states in dynamical systems are not guaranteed to jump in their entirety. For example, in mechanical systems with impacts, only higher-order states jump (*e.g.* velocities). Moreover, when the underlying dynamics is only partially observable, which is the case in numerous real-world problems (*e.g.*, only a patient’s temperature is measured), interventions cause jumps in a latent representation of the state, ultimately leading to an abrupt change in the dynamics driving the *observable*. As a result, the state does not jump, but rather continuously changes according to the new, modified underlying dynamics.

3 Proposed Approach

With the objective of alleviating the underlying limitations in NJDE-based approaches, we propose IMODE, a novel framework designed to natively accommodate various types of intervention effects, common across application areas. IMODE can properly model both the system’s autonomous dynamics as well as the effect of interventions. We first describe the mathematical framework of IMODE, followed by the discussion on how it can be applied to different types of systems.

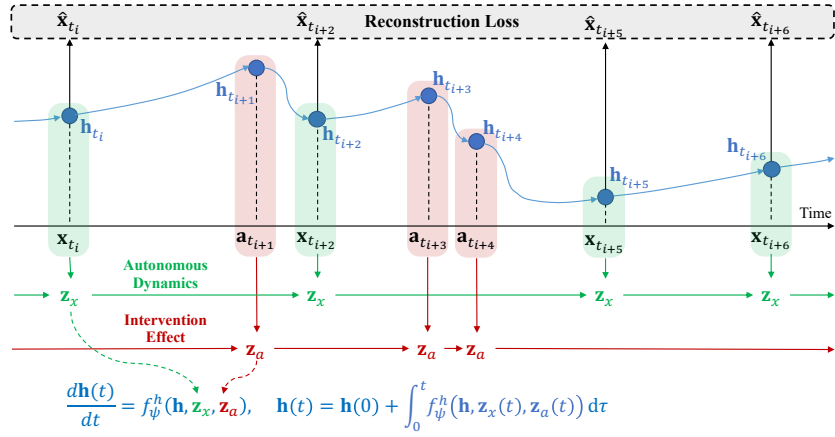


Figure 2: Overview of IMODE. \mathbf{z}_x represents the latent state of the autonomous dynamics based on observations \mathbf{x} 's and states \mathbf{h} 's, while \mathbf{z}_a represents the latent state of the intervention effect based on states \mathbf{h} 's and actions \mathbf{a} 's. f_{ψ}^h combines \mathbf{z}_x , \mathbf{z}_a , and \mathbf{h} to obtain the final system dynamics $d\mathbf{h}/dt$. We train our model via the reconstruction loss of the observations.

Model Architecture of IMODE

Notation: We use \mathbf{x}_{t_k} to denote the observation at timestep t_k , and \mathbf{a}_{t_k} to denote an intervention at timestep t_k , where $t_k \in [0, T]$, T being the end of the timeline. Therefore an observation and an intervention can occur either at the same time (*i.e.* $\mathbf{x}_{t_k}, \mathbf{a}_{t_k}$) or at different times. We use $\mathbf{X}_{0:t_k}$ to denote all observations between time zero and t_k (inclusive), and $\mathbf{A}_{0:t_k}$ to denote all interventions between time zero and t_k (inclusive). A comprehensive notation table for this section is provided in Appendix A.

IMODE Framework: Figure 2 illustrates our model architecture at a high level. Observations \mathbf{X} and interventions \mathbf{A} occur in a particular order, and the system state \mathbf{h} evolves over time. IMODE performs intervention modeling as

| | |
|---------------------|------------------------------------------------------------------------------------------------------------------------------------------------------------------------------------------------------------------------------------|
| continuous dynamics | $\begin{aligned} \dot{\mathbf{h}} &= f_{\psi}^h(\mathbf{h}, \mathbf{z}_x, \mathbf{z}_a) \\ \dot{\mathbf{z}}_x &= f_{\theta}^x(\mathbf{z}_x) \\ \dot{\mathbf{z}}_a &= f_{\phi}^a(\mathbf{z}_a) \end{aligned} \quad t \neq t_k$ |
| discrete dynamics | $\begin{aligned} \mathbf{h}^+ &= \mathbf{h} \\ \mathbf{z}_x^+ &= g_{\theta}^x(\mathbf{h}, \mathbf{z}_x, \mathbf{x}_{t_k}) \\ \mathbf{z}_a^+ &= g_{\phi}^a(\mathbf{h}, \mathbf{z}_a, \mathbf{a}_{t_k}) \end{aligned} \quad t = t_k$ |
| predictor (decoder) | $\hat{\mathbf{x}}(t) = \ell_{\omega}(\mathbf{h}(t))$ |

(3)

where f_{θ}^x, f_{ϕ}^a model the independent vector fields of autonomous latent state \mathbf{z}_x and intervention effect \mathbf{z}_a , respectively. Without external observations or interventions, the latent state \mathbf{h} evolves according to f_{ψ}^h , tasked with mixing instantaneous observation and intervention effects appropriately. This is opposed to standard Neural ODEs, where the dynamics is typically determined only by the latent system state \mathbf{h} . IMODE is further equipped with specific components to incorporate sporadic observations and interventions, namely g_{θ}^x and g_{ϕ}^a , which induce jumps on \mathbf{z}_x and \mathbf{z}_a while preserving continuity of \mathbf{h} . It is often the case that the current and the past interventions have a combined effect on the system (*i.e.* medications given to patients over time); to address such scenarios, we allow g_{θ}^x, g_{ϕ}^a to leverage information

contained in \mathbf{h} , in addition to \mathbf{z}_x and \mathbf{z}_a .

We train the various components of (3) with a reconstruction loss of the type:

$$\mathcal{L} := \frac{1}{K} \sum_{k=i}^K \|\mathbf{x}_{t_k} - \hat{\mathbf{x}}(t_k)\|_2^2 = \frac{1}{K} \sum_{k=i}^K \|\mathbf{x}_{t_k} - \ell_{\omega}(\mathbf{h}(t_k))\|_2^2 \quad (4)$$

where ℓ_{ω} is a trainable decoding function that maps \mathbf{h} back to observation space \mathbf{x} . IMODE is therefore trained by solving the following nonlinear program

$$\begin{aligned} & \min_{\psi, \theta, \phi, \omega} \frac{1}{K} \sum_{k=i}^K \|\mathbf{x}_{t_k} - \ell_{\omega}(\mathbf{h}(t_k))\|_2^2 \\ & \text{subject to } \mathbf{h}(t) = \mathbf{h}(0) + \int_0^t f_{\psi}^h(\mathbf{h}, \mathbf{z}_x(\tau), \mathbf{z}_a(\tau)) d\tau \\ & \begin{cases} \begin{bmatrix} \dot{\mathbf{z}}_x \\ \dot{\mathbf{z}}_a \end{bmatrix} = \begin{bmatrix} f_{\theta}^x(\mathbf{z}_x) \\ f_{\phi}^a(\mathbf{z}_a) \end{bmatrix} & t \neq t_k \\ \begin{bmatrix} \mathbf{z}_x^+ \\ \mathbf{z}_a^+ \end{bmatrix} = \begin{bmatrix} g_{\theta}^x(\mathbf{h}, \mathbf{z}_x, \mathbf{x}_{t_k}) \\ g_{\phi}^a(\mathbf{h}, \mathbf{z}_a, \mathbf{a}_{t_k}) \end{bmatrix} & t = t_k \end{cases} \\ & t \in [0, t_K] \end{aligned} \quad (5)$$

System-Specific Variants of IMODE

The framework of our model allows a flexible implementation depending on the property of the target system. In the following, we give a few concrete examples.

Switching intervention effect: For example, a ball in uniform motion can be seen as having constant autonomous dynamics: given no external force, it will continue to move along the same course. However, if it comes in contact with another moving ball, its direction will permanently change. In these scenarios, appropriate architectural choices for model (3) would be, as an example, those provided in Table 1. With no intervention given, the autonomous vector field f_{θ}^x is solely determined by the current state \mathbf{h}_{t_i} . If a collision occurs, the intervention latent state \mathbf{z}_a abruptly changes based on the colliding ball state, thus indirectly affecting \mathbf{h} through

| continuous dyn. | model | | discrete dyn. | model |
|-----------------|-------------------------------|--|-----------------|-------|
| f_{ψ}^h | $\mathbf{z}_x + \mathbf{z}_a$ | | g_{θ}^x | MLP |
| f_{θ}^x | 0 | | g_{ϕ}^a | MLP |
| f_{ϕ}^a | 0 | | ℓ_{ω} | Id |

Table 1: IMODE variant for switching intervention effects.

f_{ψ}^h . The intervention effect from \mathbf{z}_a is constant until a following collision happens; this, in turn, leads to a switching behavior of f_{ψ}^h aligned with intervention events.

Decaying intervention effect: For example, we can imagine a patient in an Intensive Care Unit (ICU) whose cardiovascular function is slowly deteriorating. Administering medications to this patient will have an effect that decays over time, as the ingredient is consumed by the system (*i.e.* the patient). Such a system can be modeled through the following component choices:

| continuous dyn. | model | | discrete dyn. | model |
|-----------------|------------------------|--|-----------------|-------|
| f_{ψ}^h | MLP | | g_{θ}^x | MLP |
| f_{θ}^x | MLP | | g_{ϕ}^a | MLP |
| f_{ϕ}^a | $-\alpha \mathbf{z}_a$ | | ℓ_{ω} | Id |

Table 2: IMODE variant for decaying intervention effects.

The patient’s autonomous dynamics f_{θ}^x are kept general, and incorporate new observations through g_{θ}^x . This, in turns, yields a combined effect on \mathbf{z}_x mimicking that of an ODE-RNN (Rubanova, Chen, and Duvenaud 2019). On the other hand, the latent intervention state \mathbf{z}_a is assumed to be decaying in time. We encode this prior information in the functional form of the flow f_{ϕ}^a .

Generalized Implementation: Based on two concrete examples above, we propose the most general form of IMODE that can ideally model any systems with irregular observations and interventions, without assuming prior knowledge of the autonomous dynamics and the intervention effect. Model (3) does not assume any particular functional form of intervention effects and system dynamics, making it a particularly appropriate general purpose choice.

| continuous dyn. | model | | discrete dyn. | model |
|-----------------|-------|--|-----------------|-------|
| f_{ψ}^h | MLP | | g_{θ}^x | MLP |
| f_{θ}^x | MLP | | g_{ϕ}^a | MLP |
| f_{ϕ}^a | MLP | | ℓ_{ω} | MLP |

Table 3: IMODE variant for general purpose settings.

4 Experiments

We evaluate IMODE with two simulated datasets and one real-world medical records both quantitatively and qualitatively. The two simulated datasets (Moving Ball and Exponential Decay) represent systems with permanent-effect interventions and decaying-effect interventions, respectively. We also use eICU (Pollard et al. 2018), a publicly available electronic health records, to evaluate IMODE’s performance on real-world data. Detailed experimental settings including the hyperparameters are described in Appendix B. All datasets and IMODE source code are available at GitHub¹.

Moving Ball & Exponential Decay

We use two simulated datasets, *Moving Ball* and *Exponential Decay* to demonstrate IMODE’s capability to model the first two cases described in Section 3: permanent-effect interventions, and changing autonomous dynamics with time-decaying effects of intervention. Observations \mathbf{x} and interventions \mathbf{a} in Moving Ball consist of 2D positions of the target ball, and 2D positions and 2D velocities of intervening balls, sampled from a contact simulator², where we set all balls to have the same size and mass. Example trajectories can be seen in Figure 3. Note that the velocity of the target ball is unobserved, forcing the models to infer the velocity based on positions.

In Exponential Decay, observations \mathbf{x} consist of 2D positions that follow a deterministic dynamics based on \mathbf{x} . Interventions \mathbf{a} consist of 2D values sampled from $\mathcal{N}(\mathbf{0}, \mathbf{I})$ with 10% chance at every time unit. The effect of interventions is determined by a non-linear function (*i.e.* a randomly initialized MLP with ReLU activation) using \mathbf{x} , $d\mathbf{x}/dt$ and \mathbf{a} as input. The effect is added to \mathbf{x} , and the value of an effect is halved at every time unit. Example trajectories can be seen in Figure 4. Note that the intervention effect is hidden from the model, as only the randomly sampled \mathbf{a} is given. We describe the simulation algorithm of Exponential Decay in Appendix C. In both Moving Ball and Exponential Decay, the initial position \mathbf{x}_0 and the initial velocity $d\mathbf{x}_0/dt$ are randomly chosen. For both Moving Ball and Exponential Decay, we generated 1,000 samples for training, 100 for validation, and 100 for testing, where all samples have the sequence length of 50.

Baseline Methods We compare IMODE against both RNN-based and ODE-based methods: GRU with time-gap information (GRU- Δ_t), GRU with exponentially decaying hidden states (GRU-Decay), ODE-RNN (Rubanova, Chen, and Duvenaud 2019), and GRU-ODE-Bayes (De Brouwer et al. 2019). Specifically, GRU-decay can be seen as using prior knowledge of intervention effects, similar to classical intervention models discussed in Section 5. Note that observations \mathbf{x} occur regularly (*i.e.* no missing value) but the interventions occur irregularly. To feed observations \mathbf{X} and interventions \mathbf{A} to the baseline models, we align both time-series data by the time and concatenate them. If \mathbf{a} does not exist at some timestep t_k , we set it to a zero vector. Given in-

¹<https://github.com/eogms282/IMODE>

²<https://scipython.com/blog/two-dimensional-collisions>

| Methods | Moving Ball ($\times 10^{-2}$) | | Exponential Decay ($\times 10^{-4}$) | |
|----------------------|----------------------------------|------------------------------|----------------------------------------|------------------------------|
| | Validation MSE | Test MSE | Validation MSE | Test MSE |
| GRU- Δ_t | 6.033 (± 0.272) | 5.994 (± 0.102) | 4.381 (± 2.004) | 5.686 (± 3.258) |
| GRU-Decay | 6.384 (± 0.059) | 5.994 (± 0.102) | 5.135 (± 1.660) | 6.589 (± 5.109) |
| ODE-RNN | 2.478 (± 0.142) | 2.502 (± 0.328) | 3.342 (± 1.161) | 2.778 (± 1.173) |
| GRU-ODE-Bayes | 2.506 (± 0.436) | 2.597 (± 0.520) | 3.852 (± 2.903) | 3.643 (± 4.996) |
| CRN | 2.209 (± 0.065) | 2.220 (± 0.299) | 3.716 (± 2.542) | 4.881 (± 3.846) |
| IMODE <i>switch</i> | 1.914 (± 0.173) | 1.794 (± 0.203) | 0.019 (± 0.001) | 0.027 (± 0.005) |
| IMODE <i>decay</i> | 1.794 (± 0.203) | 1.816 (± 0.203) | 0.142 (± 0.084) | 0.131 (± 0.490) |
| IMODE <i>general</i> | 1.798 (± 0.215) | 1.824 (± 0.230) | 0.039 (± 0.009) | 0.041 (± 0.008) |

Table 4: Validation and test MSE of all models on Moving Ball and Exponential Decay.

put $[\mathbf{X}_{0:t_k}; \mathbf{A}_{0:t_k}]$, RNN-based models are trained to predict $\mathbf{x}_{t_{k+1}}$.

ODE-based models are trained in the same fashion as IMODE (Eq. 4). We also test three variants of IMODE differing in terms of expressiveness: 1) IMODE *switch* from Table 1, 2) IMODE *decay* from Table 2, 3) IMODE *general* from Table 3. We also use Counterfactual Recurrent Network (CRN) (Bica et al. 2020) as a baseline, the state-of-the-art model that takes interventions into account when modeling observations. CRN, however, models only discrete interventions whereas interventions in Moving Ball and Exponential Decay are continuous. We therefore use a modified CRN (modification details are provided in Appendix D).

Quantitative Evaluation During training, we fed the first 10 true observations (*i.e.* the 2D positions) to each model, and then made it evolve for the remaining 40 steps, while always using true intervention values \mathbf{A} from time 0. Model parameters were updated via the MSE loss between the predicted observations $\hat{\mathbf{X}}$ and the true observations \mathbf{X} . The test MSEs were measured in the same fashion; given the first 10 true positions, and the true intervention information, simulate the remaining 40 steps. We conduct 5-fold cross-validation for all experiments.

As seen in Table 4, all IMODE variants consistently outperform the baseline models for both datasets. Moreover, IMODE *general* shows robust performance in both Moving Ball and Exponential Decay, demonstrating its capability to learn two significantly different dynamical systems. The performance gap between baselines and IMODE is much larger for Exponential Decay, indicating that IMODE is a suitable framework especially in modeling the system with a global pattern (*i.e.* autonomous dynamics) and local perturbations (*i.e.* interventions). It is also noteworthy that the MSEs of all models are shown to be significantly higher for Moving Ball compared to Exponential Decay, probably due to the difficulty of modeling acute changes in the ball dynamics, as seen in Figure 3.

We further tested all models in counterfactual scenarios using both datasets where a single trajectory, after 10 initial steps, divides into two alternative futures (with and without an intervention) and continues for another 10 steps. Example trajectories can be seen in Figure 5. We feed the first 10 steps to the already trained models from Table 4 and then let

| Methods | Moving Ball ($\times 10^{-2}$) | Exponential Decay ($\times 10^{-4}$) |
|----------------------|----------------------------------|----------------------------------------|
| GRU- Δ_t | 1.761 (± 0.204) | 2.014 (± 0.650) |
| GRU-Decay | 1.802 (± 0.184) | 2.289 (± 0.375) |
| ODE-RNN | 1.280 (± 0.179) | 1.771 (± 0.654) |
| GRU-ODE-Bayes | 1.318 (± 0.064) | 1.246 (± 0.451) |
| CRN | 0.682 (± 0.205) | 1.446 (± 0.498) |
| IMODE <i>switch</i> | 0.247 (± 0.017) | 0.092 (± 0.002) |
| IMODE <i>decay</i> | 0.222 (± 0.035) | 0.082 (± 0.003) |
| IMODE <i>general</i> | 0.221 (± 0.035) | 0.094 (± 0.003) |

Table 5: Test MSEs of all models in counterfactual scenarios (alternative futures) using two datasets.

them simulate the next 10 steps for two alternative futures. As seen from Table 5, IMODE variants again outperform all baselines in these counterfactual scenarios. The fact that IMODE is able to separately learn autonomous dynamics and intervention effects clearly indicates its capability to generalize to alternative cases.

Model Behavior Analysis To confirm that IMODE properly learns the autonomous dynamics and the intervention effect, we visualize test trajectories from Moving Ball (Figure 3) and Exponential Decay (Figure 4), where the first 10 true timesteps are given to the model, and the model simulates the remaining 40 steps while using true interventions. We show the results of IMODE *general*, ODE-RNN, and RNN-Decay for comparison. In both figures, IMODE clearly outperforms baseline models as it closely follows the true trajectories, while the baselines often diverge. The comparison between Figures 3 and 4 demonstrates the challenging nature of Moving Ball, thus resulting in the higher MSE in Table 4. Whereas Exponential Decay shows smooth and moderate change of dynamics, the changes in Moving Ball are not only discrete but also significant (*e.g.*, ball changing direction in almost 180 degrees).

Figure 3 shows that the autonomous latent state \mathbf{z}_x stays rather static, while the intervention latent state \mathbf{z}_a jumps when a collision occurs. One can also see from this figure that after the jump, \mathbf{z}_a does not decay over time, indicating that IMODE is successfully recording the permanent effects of all the previous interventions. Ideally, \mathbf{z}_x should remain constant over time, but minor changes and fluctuations are found, especially in the second trajectory of Figure 3, leaving

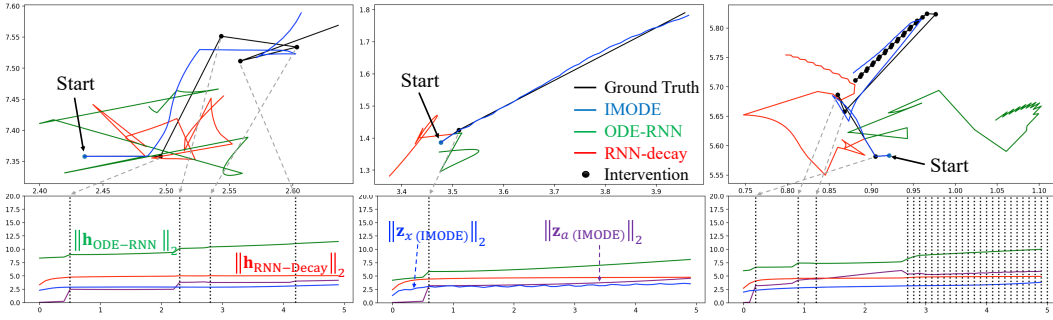


Figure 3: Simulated trajectories and L_2 norms of latent states of IMODE and baselines for the Moving Ball dataset. The gray dotted lines connects collision points to the corresponding timesteps. The three samples represent medium, light, and heavy interventions, respectively.

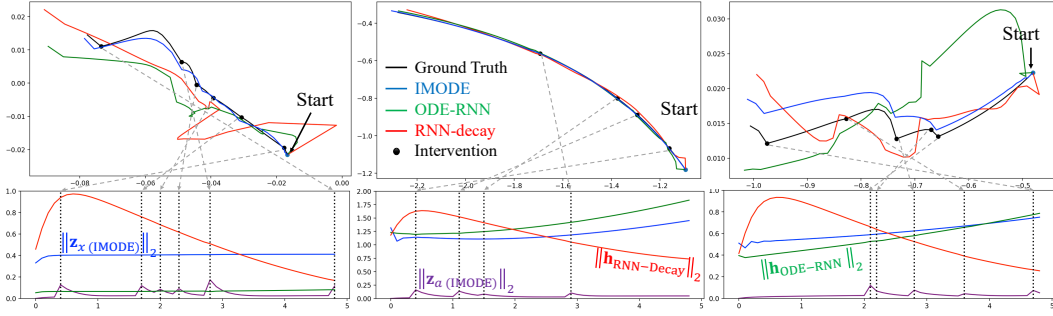


Figure 4: Simulated trajectories and L_2 norms of latent states of IMODE and baselines for the Exponential Decay dataset. The gray dotted lines connects intervention points to the corresponding timesteps. The three samples represent medium, light, and heavy interventions, respectively.

room for further improvement. Based on the trajectories of $\|\mathbf{h}_{\text{ODE-RNN}}\|_2$, ODE-RNN also recognizes the occurrence of collisions, but it fails to treat observations and interventions separately, leading to incorrect simulation. Compared to Moving Ball, Exponential Decay is a completely different system where the state follows its own dynamics while being occasionally perturbed with an exponentially decaying effect. Thanks to its relatively smooth trajectory, even the baseline models tend to stay close to the true trajectory. However, the L_2 norm plots of Figure 4 clearly demonstrates the benefit of separately modeling observations and interventions. While $\|z_x\|_2$ demonstrates a smoothly changing trajectory potentially corresponding to the autonomous system dynamics, $\|z_a\|_2$ jumps when an intervention occurs and decays over time, indicating that IMODE has properly learned the true intervention effect on the system.

We also provide visual examples for the counterfactual scenarios. The two figures in Figure 5 describe two counterfactual cases in Moving Ball and Exponential Decay respectively. As indicated by the quantitative results in Table 5, IMODE outperforms baseline models in both datasets, as it closely follows the two alternative futures while the baselines diverge from the true trajectories in both alternative cases.

eICU Dataset

The eICU Collaborative Research Database (eICU) (Polard et al. 2018) contains publicly available electronic health

records (EHR) collected from multiple intensive care units (ICU). In order to correctly evaluate IMODE’s ability to learn the patient’s autonomous dynamics and the effect of interventions (*i.e.* drugs), we choose a patient with the longest ICU stay whose drugs were given only via IV infusion to remove any confounding factors (*e.g.*, drugs taken orally). We focus on a single patient since every patient has a unique autonomous dynamics and response to drugs determined by hidden factors (*e.g.*, DNA and diet). We leave handling multiple heterogeneous dynamics with a single model as future work. We extract from the EHR three blood pressure features (systolic, diastolic, and mean) measured every 5 minutes as the observation \mathbf{x} , and the hourly interventions a consist of five drug types (norepinephrine, vasopressin, propofol, amiodarone, and phenylephrine) and their dosage. We binned the entire observations into 2.5-hour buckets (30 timesteps containing two interventions) and used 150 buckets for training, 50 for validation and 50 for testing.

Quantitative Evaluation Using the same set of baselines as in the above experiments, we train all models with the reconstruction loss (Eq. 4) in a similar fashion as before; 6 true timesteps are given to the models, and the remaining 24 steps are simulated using true intervention information. We conduct 5-fold cross validation for all models. As can be seen in Table 6, IMODE shows the best test performance, demonstrating its potential applicability to real-world data such as patient vital signs. We also present further analysis of the model behavior in Appendix E.

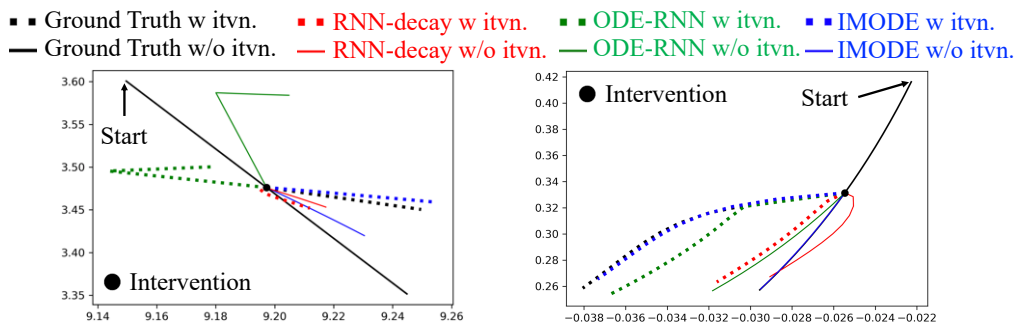


Figure 5: (Left) Simulated trajectories of IMODE and baselines for Moving Ball. 10 steps are simulated before trajectory divides into two alternative futures. (Right) Simulated trajectories of IMODE and baselines for Exponential Decay. In the same manner, 10 steps are simulated before trajectory divides into two alternative futures.

| Methods | Validation MSE ($\times 10^{-3}$) | Test MSE ($\times 10^{-3}$) |
|----------------------|-------------------------------------|-------------------------------|
| GRU- Δ_t | 6.010 (± 0.337) | 6.061 (± 1.099) |
| GRU-Decay | 6.789 (± 0.374) | 6.899 (± 0.445) |
| ODE-RNN | 4.234 (± 0.337) | 4.414 (± 0.412) |
| GRU-ODE-Bayes | 5.588 (± 1.258) | 5.988 (± 1.350) |
| CRN | 5.551 (± 1.193) | 5.771 (± 1.125) |
| IMODE <i>switch</i> | 6.437 (± 3.332) | 6.410 (± 3.056) |
| IMODE <i>decay</i> | 4.262 (± 0.355) | 4.245 (± 0.250) |
| IMODE <i>general</i> | 4.047 (± 0.255) | 4.209 (± 0.308) |

Table 6: Validation and test MSE of all models on eICU.

5 Related Work

Continuous-Depth Learning Continuous-depth learning (Sonoda and Murata 2017; Haber and Ruthotto 2017; Hauser and Ray 2017; Lu et al. 2017; Che et al. 2018; Massaroli et al. 2020b) has recently emerged as a novel paradigm providing a dynamical system perspective on machine learning. This view has inspired design of novel architectures (Chang et al. 2017; Zhu, Chang, and Fu 2018; Demeester 2019; Chang et al. 2019; Cranmer et al. 2020; Massaroli et al. 2020a) as well as guiding the injection of physics-inspired inductive biases (Greydanus, Dzamba, and Yosinski 2019; Köhler, Klein, and Noé 2019). The framework has seen applications to various classes of differential equations (Tzen and Raginsky 2019; Li et al. 2020) and graphs (Poli et al. 2019), along with several analyses regarding computational speedups through regularization (Finlay et al. 2020) or specific numerical methods (Poli et al. 2020).

(Rubanova, Chen, and Duvenaud 2019) demonstrated promising empirical performance across various forecasting datasets by combining RNNs with Neural ODEs. (Yildiz, Heinonen, and Lahdesmaki 2019) refined the architecture through higher-order dynamics and Bayesian networks. (De Brouwer et al. 2019) alternates a filtering and predictions steps to improve performance in settings with highly sporadic observations. (Jia and Benson 2019) models a stochastic event by estimating the occurrence probability with Neural ODEs, where a new event observation updates the event intensity. While the above approaches share similarities with the proposed approach such that a input sequence modifies

the internal state, they fail to treat observations and interventions differently, leading to suboptimal performance when modeling external interventions in a given system.

Intervention Modeling Intervention modeling is typically discussed in the context of time-series analysis. Combining the intervention analysis technique with the classical time-series models enables the user to handle time-series data with different types of interventions such as permanent, gradually increasing or decreasing, and complex effects (Glass, Willson, and Gottman 2008). Intervention analysis has been used across diverse domains such as healthcare (Evans 2002; Wagner et al. 2002), economics (Box and Tiao 1975) and policies (Enders and Sandler 1993). More recent studies have been conducted in the context of patient modeling, where models based on a Gaussian Process (GP) and RNNs have been proposed (Schulam and Saria 2017; Soleimani, Subbaswamy, and Saria 2017; Lim 2018; Bica et al. 2020). Considering the restricted model structure that GP assumes, we used the state-of-the-art patient modeling algorithm from Bica et al. as one of the baselines. Causal analysis is also relevant to our work, but it aims to identify the causal relationship between input (usually a mixture of causal factors and confounders) and output (Pearl 2009). On the other hand, intervention modeling focuses on correctly predicting the effect of an external force. As intervention modeling is essentially a time-series problem, Neural ODEs are a natural framework for this task.

6 Conclusions

In this work, we proposed IMODE, a Neural ODE-based framework that can properly model dynamical systems with external interventions. IMODE employs two components where one models the autonomous dynamics of the system, and the other models the intervention effect on the system. Using both simulated and real-world datasets, we quantitatively demonstrated IMODE’s superiority in intervention modeling, as well as in-depth analysis on its behavior. As future work, we plan to apply IMODE in large-scale real-world datasets while extending IMODE to further disentangle the autonomous dynamics and the intervention effects.

Ethical Impact

Although we empirically demonstrated that the proposed framework IMODE is capable of learning separate latent states for both autonomous dynamics and intervention effects, it should be used with caution in real-world applications. As described in Section 5, IMODE is not a causal analysis model, which means that the user must possess domain knowledge as to which variables are observations and which are interventions, and that there are no unobserved confounders that can affect the given dynamical system (as described in the eICU Dataset subsection). For example, we believe IMODE can be used to model patient status in a well-controlled environment such as patients under anesthesia during operation. We are certain more opportunities will follow as we address issues such as scalability and confounding factors in the future.

References

- Baytas, I. M.; Xiao, C.; Zhang, X.; Wang, F.; Jain, A. K.; and Zhou, J. 2017. Patient subtyping via time-aware LSTM networks. In *Proceedings of the 23rd ACM SIGKDD international conference on knowledge discovery and data mining*, 65–74.
- Bica, I.; Alaa, A. M.; Jordon, J.; and van der Schaar, M. 2020. Estimating counterfactual treatment outcomes over time through adversarially balanced representations. In *International Conference on Learning Representation*.
- Box, G. E.; and Tiao, G. C. 1975. Intervention analysis with applications to economic and environmental problems. *Journal of the American Statistical association* 70(349): 70–79.
- Chang, B.; Chen, M.; Haber, E.; and Chi, E. H. 2019. AntisymmetricRNN: A dynamical system view on recurrent neural networks. *arXiv preprint arXiv:1902.09689*.
- Chang, B.; Meng, L.; Haber, E.; Tung, F.; and Begert, D. 2017. Multi-level residual networks from dynamical systems view. *arXiv preprint arXiv:1710.10348*.
- Che, Z.; Purushotham, S.; Cho, K.; Sontag, D.; and Liu, Y. 2018. Recurrent neural networks for multivariate time series with missing values. *Scientific reports* 8(1): 1–12.
- Chen, T. Q.; Rubanova, Y.; Bettencourt, J.; and Duvenaud, D. K. 2018. Neural ordinary differential equations. In *Advances in neural information processing systems*, 6571–6583.
- Cho, K.; Van Merriënboer, B.; Gulcehre, C.; Bahdanau, D.; Bougares, F.; Schwenk, H.; and Bengio, Y. 2014. Learning phrase representations using RNN encoder-decoder for statistical machine translation. *arXiv preprint arXiv:1406.1078*.
- Choi, E.; Bahadori, M. T.; Schuetz, A.; Stewart, W. F.; and Sun, J. 2016. Doctor ai: Predicting clinical events via recurrent neural networks. In *Machine Learning for Healthcare Conference*, 301–318.
- Cranmer, M.; Greydanus, S.; Hoyer, S.; Battaglia, P.; Spergel, D.; and Ho, S. 2020. Lagrangian neural networks. *arXiv preprint arXiv:2003.04630*.
- De Brouwer, E.; Simm, J.; Arany, A.; and Moreau, Y. 2019. GRU-ODE-Bayes: Continuous modeling of sporadically-observed time series. In *Advances in Neural Information Processing Systems*, 7377–7388.
- Demeester, T. 2019. System Identification with Time-Aware Neural Sequence Models. *arXiv preprint arXiv:1911.09431*.
- Du, N.; Dai, H.; Trivedi, R.; Upadhyay, U.; Gomez-Rodriguez, M.; and Song, L. 2016. Recurrent marked temporal point processes: Embedding event history to vector. In *Proceedings of the 22nd ACM SIGKDD International Conference on Knowledge Discovery and Data Mining*, 1555–1564.
- Enders, W.; and Sandler, T. 1993. The effectiveness of antiterrorism policies: A vector-autoregression-intervention analysis. *American Political Science Review* 87(4): 829–844.
- Evans, D. 2002. The effectiveness of music as an intervention for hospital patients: a systematic review. *Journal of advanced nursing* 37(1): 8–18.
- Finlay, C.; Jacobsen, J.-H.; Nurbekyan, L.; and Oberman, A. M. 2020. How to train your neural ODE. *arXiv preprint arXiv:2002.02798*.
- Glass, G. V.; Willson, V. L.; and Gottman, J. M. 2008. *Design and analysis of timeseries experiments*. IAP.
- Greydanus, S.; Dzamba, M.; and Yosinski, J. 2019. Hamiltonian neural networks. In *Advances in Neural Information Processing Systems*, 15353–15363.
- Haber, E.; and Ruthotto, L. 2017. Stable architectures for deep neural networks. *Inverse Problems* 34(1): 014004.
- Hauser, M.; and Ray, A. 2017. Principles of Riemannian geometry in neural networks. In *Advances in neural information processing systems*, 2807–2816.
- Jia, J.; and Benson, A. R. 2019. Neural jump stochastic differential equations. In *Advances in Neural Information Processing Systems*, 9843–9854.
- Köhler, J.; Klein, L.; and Noé, F. 2019. Equivariant Flows: sampling configurations for multi-body systems with symmetric energies. *arXiv preprint arXiv:1910.00753*.
- Kulev, G.; and Bainov, D. 1988. Strong stability of impulsive systems. *International journal of theoretical physics* 27(6): 745–755.
- Lakshmikantham, V.; Simeonov, P. S.; et al. 1989. *Theory of impulsive differential equations*, volume 6. World scientific.
- Li, X.; Wong, T.-K. L.; Chen, R. T.; and Duvenaud, D. 2020. Scalable Gradients for Stochastic Differential Equations. *arXiv preprint arXiv:2001.01328*.
- Lim, B. 2018. Forecasting treatment responses over time using recurrent marginal structural networks. In *Advances in Neural Information Processing Systems*, 7483–7493.
- Lipton, Z. C.; Kale, D.; and Wetzel, R. 2016. Directly modeling missing data in sequences with rnns: Improved classification of clinical time series. In *Machine Learning for Healthcare Conference*, 253–270.
- Lu, Y.; Zhong, A.; Li, Q.; and Dong, B. 2017. Beyond finite layer neural networks: Bridging deep architectures and numerical differential equations. *arXiv preprint arXiv:1710.10121*.
- Massaroli, S.; Poli, M.; Bin, M.; Park, J.; Yamashita, A.; and Asama, H. 2020a. Stable Neural Flows. *arXiv preprint arXiv:2003.08063*.
- Massaroli, S.; Poli, M.; Park, J.; Yamashita, A.; and Asama, H. 2020b. Dissecting neural odes. *arXiv preprint arXiv:2002.08071*.
- Pearl, J. 2009. *Causality*. Cambridge university press.
- Poli, M.; Massaroli, S.; Park, J.; Yamashita, A.; Asama, H.; and Park, J. 2019. Graph Neural Ordinary Differential Equations. *arXiv preprint arXiv:1911.07532*.

- Poli, M.; Massaroli, S.; Yamashita, A.; Asama, H.; and Park, J. 2020. Hypersolvers: Toward Fast Continuous-Depth Models. *arXiv preprint arXiv:2007.09601* .
- Pollard, T. J.; Johnson, A. E.; Raffa, J. D.; Celi, L. A.; Mark, R. G.; and Badawi, O. 2018. The eICU Collaborative Research Database, a freely available multi-center database for critical care research. *Scientific data* 5: 180178.
- Rubanova, Y.; Chen, T. Q.; and Duvenaud, D. K. 2019. Latent Ordinary Differential Equations for Irregularly-Sampled Time Series. In *Advances in Neural Information Processing Systems*, 5321–5331.
- Schulam, P.; and Saria, S. 2017. Reliable decision support using counterfactual models. In *Advances in Neural Information Processing Systems*, 1697–1708.
- Soleimani, H.; Subbaswamy, A.; and Saria, S. 2017. Treatment-response models for counterfactual reasoning with continuous-time, continuous-valued interventions. In *UAI*.
- Sonoda, S.; and Murata, N. 2017. Double continuum limit of deep neural networks. In *ICML Workshop Principled Approaches to Deep Learning*.
- Tzen, B.; and Raginsky, M. 2019. Neural stochastic differential equations: Deep latent gaussian models in the diffusion limit. *arXiv preprint arXiv:1905.09883* .
- Wagner, A. K.; Soumerai, S. B.; Zhang, F.; and Ross-Degnan, D. 2002. Segmented regression analysis of interrupted time series studies in medication use research. *Journal of clinical pharmacy and therapeutics* 27(4): 299–309.
- Yildiz, C.; Heinonen, M.; and Lahdesmaki, H. 2019. ODE2VAE: Deep generative second order ODEs with Bayesian neural networks. In *Advances in Neural Information Processing Systems*, 13412–13421.
- Zhu, M.; Chang, B.; and Fu, C. 2018. Convolutional neural networks combined with runge-kutta methods. *arXiv preprint arXiv:1802.08831* .

A Notation Table

Table 7 describes the notations and their descriptions used throughout this paper.

B Hyperparameters

In the experiments section, we evaluated five baseline methods: RNN- Δ_t , RNN-Decay, ODE-RNN, GRU-ODE-Bayes and CRN. We trained all baseline models for the same number of epochs in each experiment, and the final models were chosen by the validation loss in each epoch. Additionally, we trained all ODE-based models using the Runge-Kutta fourth-order method and the same delta-times.

Hyperparameters for IMODE In the Moving Ball task, we used the batch size of 32 for 1,000 epochs. When using RNNs or ODE-RNNs for both f_θ^x and f_ϕ^a , the size of the hidden vector was 40. Additionally, when using ODE-RNNs for f_θ^x and f_ϕ^a , their derivative functions were a two-layer MLP with the hidden size of 40 and LeakyReLU as the activation function. For f_ψ^h , we used the same 40-dimensional two-layer MLP with LeakyReLU activation. We used the RMSprop optimizer with the learning rate of 0.001 and set the delta-time as 0.01. In Exponential Decay, we used the same setting as Moving Ball but used 1500 epochs.

In the eICU task, we trained for 1,500 epochs with the batch size of 32. We used ODE-RNNs for the functions f_θ^x and f_ϕ^a with 20-dimensional and 10-dimensional hidden vectors respectively. For f_ψ^h , we used the 20-dimensional two-layer MLP with LeakyReLU activation. We used the delta-time of 1.0 for the ODE solver.

Baselines For the baselines in our experiments, we follow the general structure and hyperparameters of each model’s available implementation^{3,4,5,6} other than small details. Specifically, the models were tuned by the performance in the validation phase in order to obtain the proper batch size and learning rate. We also adjusted the hidden vector dimension of the baseline models to match that of IMODE.

C Algorithm of Exponential Decay

Algorithm 1 describes the pseudo-code for generating simulated samples used in the Exponential Decay task.

D Modification to Counterfactual Recurrent Network

Counterfactual Recurrent Network (CRN) (Bica et al. 2020) has Gradient Reversal Layer (GRL) that suppresses the correct prediction of the treatment type that occurs in the next timestep. This technique cannot be used in Moving Ball and Exponential Decay, because the interventions in those datasets consist of continuous values (*i.e.*, position and velocities of the incoming ball in Moving Ball, and the randomly generated intervention effect in Exponential Decay). Although the GRL component is able to predict *No Treatment* class as well, since the interventions occur randomly in Moving Ball and Exponential Decay, predicting the binary case of *Treatment* and *No Treatment* cannot be done either. Therefore, in the two simulated datasets (Moving Ball and Exponential Decay) that have continuous and unpredictable interventions, we used CRN with $\lambda = 0$ (*i.e.*, not using a treatment classifier and GRL).

³https://github.com/YuliaRubanova/latent_ode

⁴https://github.com/edebrouwer/gru_ode_bayes

⁵<https://github.com/zhiyongc/GRU-D>

⁶<https://github.com/ioanabica/Counterfactual-Recurrent-Network>

Algorithm 1 The simulation algorithm of Exponential Decay

```
1: Input: time unit  $dt$ , length of time series  $K$ 
2: Initialize observation  $\mathbf{x}_0$ ,  $d\mathbf{x}_0/dt$  are randomly chosen
   in  $[0, 1]$ , intervention effect  $e_0 = 0$ ,
   update matrix of dynamics  $(d\mathbf{x}/dt) M_v = \begin{bmatrix} 1.5 & 0 \\ 0 & -2.5 \end{bmatrix}$ 
3: for  $k = 1$  to  $K$  do
4:    $a_k = 0$ 
5:    $\mathbf{x}_k = \mathbf{x}_{k-1} + dt * (d\mathbf{x}_{k-1}/dt + e_{k-1})$ 
6:    $d\mathbf{x}_k/dt = M_v(d\mathbf{x}_{k-1}/dt)$ 
7:    $e_k = e_{k-1} * 0.5$ 
8:    $intervention\_occurs \sim Bernoulli(0.1)$ 
9:   if  $intervention\_occurs$  then
10:     $a_k \sim \mathcal{N}(0, 1)$ 
11:     $e_k = e_k + MLP([\mathbf{x}_k, d\mathbf{x}_k/dt, a_k])$ 
12:   end if
13: end for
14: return  $\mathbf{X}_{1:K}, \mathbf{A}_{1:K}$ 
```

In the eICU experiment, although the value of intervention is continuous (*i.e.*, the dosage of each treatment), their treatment type and its administration time would be predictable using observational trajectories of patient. Therefore, as the original setting in CRN, we used a treatment classifier to predict treatment types excluding their dosage. Additionally, since the patients can be given multiple treatments simultaneously in the eICU experimental settings, we used the sigmoid activation function in the last layer of the treatment classifier instead of softmax function to predict the multiple treatments at the same time.

E Model Behavior Analysis for eICU

In this section, we visualize the trajectories of eICU samples and their L_2 norms to study the model behaviors. In Figure 6, the model was given true observations and interventions for the first six steps. Then, each model autoregressively predicted the observations for the remaining 24 timesteps while using true interventions.

As depicted in both Figure 6 and 7, the blood pressure features seem to increase after the injection of norepinephrine which has a direct influence to rise of blood pressure, but the exact effect varies by the patient. IMODE most accurately predicts the blood pressure trajectories and effects of treatments. We found systolic blood pressure to be more unpredictable than mean blood pressure and diastolic blood pressure (for all models), as they demonstrated seemingly random trajectories, suggesting that there exist other unknown factors affecting the patients besides the medications.

As can be seen from the L_2 norm activities in both figures, IMODE successfully disentangles the autonomous dynamics of the patient and the intervention effect, where $\|\mathbf{z}_x\|_2$ demonstrates a rather stable trajectory while $\|\mathbf{z}_a\|_2$ spikes when there are interventions followed by a gradual decay.

References

Bica, I.; Alaa, A. M.; Jordon, J.; and van der Schaar, M. 2020. Estimating counterfactual treatment outcomes over time through adversarially balanced representations. In *International Conference on Learning Representation*.

| Symbol | Description | Domain (and codomain) |
|----------------|-----------------------------------|--------------------------------------------------------------------------------------------------------------------------------------|
| \mathbf{x} | input | \mathbb{R}^{n_x} |
| \mathbf{a} | intervention | \mathbb{R}^{n_a} |
| \mathbf{h} | continuous latent state | \mathbb{R}^{n_h} |
| \mathbf{z}_x | autonomous latent state | $\mathbb{R}^{n_{z,x}}$ |
| \mathbf{z}_a | intervention latent state | $\mathbb{R}^{n_{z,a}}$ |
| ψ | \mathbf{h} 's dyn. parameters | \mathbb{R}^{n_ψ} |
| θ | \mathbf{z}_x 's dyn. parameters | \mathbb{R}^{n_θ} |
| ϕ | \mathbf{z}_a 's dyn. parameters | \mathbb{R}^{n_ϕ} |
| ω | decoder's parameters | \mathbb{R}^{n_ω} |
| f_ψ^h | \mathbf{h} 's flow map | $\mathbb{R}^{n_h} \times \mathbb{R}^{n_{z,x}} \times \mathbb{R}^{n_{z,a}} \times \mathbb{R}^{n_\psi} \rightarrow \mathbb{R}^{n_h}$ |
| f_θ^x | \mathbf{z}_x 's flow map | $\mathbb{R}^{n_h} \times \mathbb{R}^{n_{z,x}} \times \mathbb{R}^{n_\theta} \rightarrow \mathbb{R}^{n_{z,x}}$ |
| f_ϕ^a | \mathbf{z}_a 's flow map | $\mathbb{R}^{n_h} \times \mathbb{R}^{n_{z,a}} \times \mathbb{R}^{n_\phi} \rightarrow \mathbb{R}^{n_{z,a}}$ |
| g_θ^x | \mathbf{z}_x 's jump map | $\mathbb{R}^{n_h} \times \mathbb{R}^{n_{z,x}} \times \mathbb{R}^{n_x} \times \mathbb{R}^{n_\theta} \rightarrow \mathbb{R}^{n_{z,x}}$ |
| g_ϕ^a | \mathbf{z}_a 's jump map | $\mathbb{R}^{n_h} \times \mathbb{R}^{n_{z,a}} \times \mathbb{R}^{n_a} \times \mathbb{R}^{n_\phi} \rightarrow \mathbb{R}^{n_{z,a}}$ |
| ℓ_ω | output decoder | $\mathbb{R}^{n_h} \times \mathbb{R}^{n_\omega} \rightarrow \mathbb{R}^{n_x}$ |

Table 7: Notations used throughout the paper.

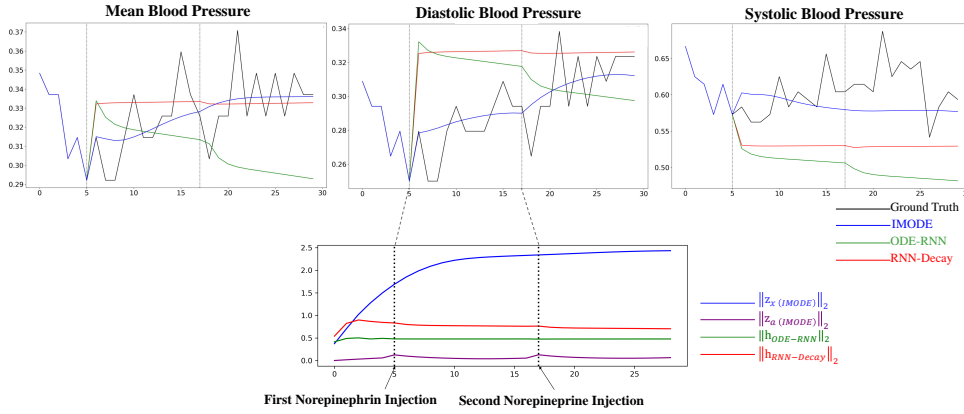


Figure 6: Three trajectories (mean blood pressure, diastolic blood pressure, and systolic blood pressure) and L_2 norms of hidden layers of IMODE and baselines for the eICU dataset. The gray-dotted lines connect intervention points (*i.e.* when norepineprine was injected) to the corresponding timesteps.

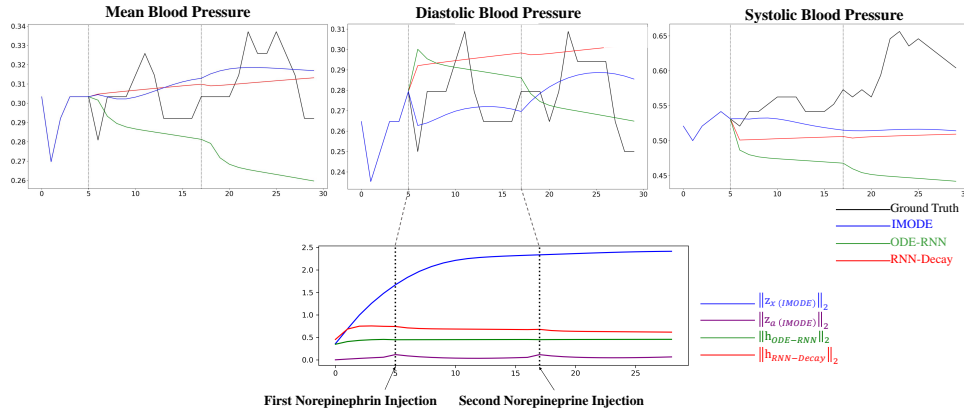


Figure 7: Another set of three trajectories (mean blood pressure, diastolic blood pressure, and systolic blood pressure) and L_2 norms of hidden layers of IMODE and baselines for the eICU dataset. The gray-dotted lines connect intervention points (*i.e.* when norepineprine was injected) to the corresponding timesteps.